

Breast cancer neoantigens can induce CD8⁺ T-cell responses and antitumor immunity

Xiuli Zhang¹, Samuel Kim¹, Jasreet Hundal², John M. Herndon¹, Shunqiang Li³, Allegra A. Petti², Savas D. Soysal^{1,6}, Lijin Li¹, Mike D. McLellan², Jeremy Hoog³, Tina Primeau³, Nancy Myers¹, Tammi L. Vickery⁷, Mark Sturmoski¹, Ian S. Hagemann⁴, Chris A. Miller^{2,3}, Matthew J. Ellis^{3,5}, Elaine R. Mardis^{2,3}, Ted Hansen⁴, Timothy P. Fleming¹, S. Peter Goedegebuure¹, and William E. Gillanders^{1,8*}

*Corresponding author

Address correspondence to William E. Gillanders, Department of Surgery, Washington University in St. Louis, 660 South Euclid Avenue, Box 8109, St. Louis, MO 63110, USA.
E-mail address: gillandersw@wudosis.wustl.edu

¹ Department of Surgery, Washington University School of Medicine, 660 South Euclid Avenue, St Louis, Missouri 63110, USA

² McDonnell Genome Institute, Washington University School of Medicine, 4444 Forest Park Avenue, St. Louis, Missouri 63108, USA

³ Department of Medicine, Division of Oncology, Washington University School of Medicine, 660 South Euclid Avenue, St. Louis, Missouri 63110, USA

⁴ Department of Pathology and Immunology, Washington University School of Medicine, 660 south Euclid Avenue, St Louis, Missouri 63110, USA

⁵ Lester and Sue Smith Breast Care Center, Oncology/Medicine and MCB, Baylor College of Medicine, One Baylor Plaza, Houston, TX 77030, USA

⁶ Department of Surgery, University Hospital Basel, Schoenbeinstrasse 40, CH-4031, Basel, Switzerland

⁷ Center for Human Immunology and Immunotherapy Programs, Washington University School of Medicine, St. Louis, Missouri.

⁸ The Alvin J. Siteman Cancer Center at Barnes-Jewish Hospital and Washington University School of Medicine, St. Louis, Missouri

Running Title: Breast cancer neoantigens can induce antitumor immunity

Keywords: breast cancer, neoantigens, T cells, immunotherapy

Grant support: This work is supported by grants to W.E.G. from Susan G. Komen for the Cure (KG111025), NCI T32 CA 009621, NIH P30CA091842, the Siteman Cancer Center/Barnes-

Jewish Hospital Foundation Cancer Frontier Fund (BJHF CFF 7538-55), and the Siteman Cancer Center Siteman Investment Program (SIP Pre-SPORE 3781).

Disclosure of Potential Conflicts of Interest: The authors declare no potential conflicts of interest.

5,767 words, 2 Figures, 1 Table, 4 Supplementary Figures, 9 Supplementary tables (including 3 excel files).

1 ABSTRACT

2 Next-generation sequencing technologies have provided insights into the biology and mutational
3 landscape of cancer. Here we evaluate the relevance of cancer neoantigens in human breast
4 cancers. Using patient-derived xenografts from three patients with advanced breast cancer
5 (xenografts were designated as WHIM30, WHIM35, and WHIM37), we sequenced exomes of
6 tumor and patient-matched normal cells. We identified 2091 (WHIM30), 354 (WHIM35), and
7 235 (WHIM37) nonsynonymous somatic mutations. A computational analysis identified and
8 prioritized HLA class I–restricted candidate neoantigens expressed in the dominant tumor clone.
9 Each candidate neoantigen was evaluated using peptide-binding assays, T-cell cultures that
10 measure the ability of CD8⁺ T cells to recognize candidate neoantigens, and preclinical models
11 in which we measured antitumor immunity. Our results demonstrate that breast cancer
12 neoantigens can be recognized by the immune system, and that human CD8⁺ T cells enriched for
13 prioritized breast cancer neoantigens were able to protect mice from tumor challenge with
14 autologous patient-derived xenografts. We conclude that next-generation sequencing and
15 epitope-prediction strategies can identify and prioritize candidate neoantigens for immune
16 targeting in breast cancer.

17 **INTRODUCTION**

18 Next-generation sequencing technologies have transformed our understanding of how somatic
19 mutations contribute to cancer initiation and progression. Improvements in instrument
20 performance together with cost reductions have enabled a systematic analysis of the mutational
21 landscape in a variety of cancer types. The results provide opportunities to personalize therapy.
22 In preclinical models, cancer neoantigens can be identified by next-generation sequencing, and
23 neoantigens can be prioritized by epitope prediction algorithms. Some neoantigens are targets for
24 checkpoint blockade therapy and personalized vaccine therapy (1-3). Ongoing clinical trials
25 confirm the importance of cancer neoantigens in the response to therapies based on immune
26 checkpoint inhibitors or personalized vaccines in non-small cell lung cancer, melanoma, and
27 colorectal cancers with DNA mismatch repair deficiency (4-9). Here we explored neoantigens in
28 breast cancer, which generally does not carry a high mutational load.

29 MATERIALS AND METHODS

30 **Human subjects.** All human subjects' research was reviewed and approved by the Human
31 Subjects Committee at Washington University School of Medicine. Three advanced stage breast
32 cancer patients participated in these studies. Each subject consented to tissue banking and
33 establishment of patient-derived xenografts (PDXs). PDXs were established in NSG mice (10)
34 and early generation tumors were flash frozen. Each subject also consented to leukapheresis. The
35 subjects were designated WHIM30, WHIM35 and WHIM37 based on the designation of their
36 PDX. Leukapheresis was performed at Barnes Jewish Hospital. Peripheral blood mononuclear
37 cells (PBMC) were isolated through density centrifugation using Ficoll-Paque PLUS, and
38 cryopreserved as cell pellets. Each subject consented to genome sequencing. Aliquots of PBMC
39 were frozen as cell pellets. DNA from PDX tumors and PBMC was extracted using the QIAamp
40 DNA Mini Kit (Qiagen Sciences, Baltimore, MD) and RNA from PDX tumors was extracted
41 using the High Pure RNA Paraffin kit (Roche, Indianapolis, IN). DNA and RNA quality was
42 determined using a Nanodrop 2000 and quantitated using a Qubit Fluorometer (Life
43 Technologies, Carlsbad, CA).

44
45 **Exome sequencing.** For each subject, tumor and normal matched DNA samples were processed
46 for whole exome sequencing using standard protocols for Kapa Biosystems NGS libraries with
47 corresponding barcoded adapters. The libraries were quantitated and combined at equimolar
48 ratios into an exome capture using the Roche Nimblegen EZ Exome version 3.0 reagent. Exome
49 sequence data were generated as 2 x 100 bp read pairs on an Illumina HiSeq2000 instrument.
50 Our Genome Modeling System (GMS) (11) was used to align exome reads and identify somatic
51 variants. The analysis pipeline uses BWA (version 0.5.9) (12) for alignment with default

52 parameters except for the following: ‘-t 4 -q 5’. All alignments were against GRCh37-lite-
53 build37 of the human reference genome and were merged and subsequently de-duplicated with
54 Picard (version 1.46). Detection of somatic mutations was performed using a combination of
55 different variant callers, including SAMtools (13,14), Somatic Sniper (15), VarScan Somatic
56 (16,17) and Strelka (18).

57
58 ***cDNA-capture sequencing.*** All RNA samples were DNase-treated with a TURBO DNA-free kit
59 (Invitrogen) as per the manufacturer’s instructions. RNA integrity and concentration were
60 assessed using an Agilent Eukaryotic Total RNA 6000 assay (Agilent Technologies) and a
61 Quant-iT™ RNA assay kit on a Qubit™ Fluorometer (Life Technologies Corporation). The
62 MicroPoly(A)Purist™ Kit (Ambion) was used to enrich for poly(A) RNA from three WHIM
63 patients DNase-treated total RNA, and the resulting RNA was converted to cDNA using the
64 Ovation® RNA-Seq System V2 (NuGen, 20 ng of either total or polyA RNA). All NuGen
65 cDNA sequencing libraries were generated using NEBNext® Ultra™ DNA Library Prep Kit
66 for Illumina® as described previously (19). Each library ligation reaction was PCR-optimized
67 using the Eppendorf Epigradient S qPCR instrument, and PCR-amplified for limited cycle
68 numbers based on the Ct value identified in the optimization step. Libraries were quantitated
69 using the Quant-iT™ dsDNA HS Assay (Life Technologies) and for size using the BioAnalyzer
70 2100 (Agilent Technologies). The Illumina-ready libraries were enriched using the Nimblegen
71 SeqCap EZ Human Exome Library v3.0 reagent. Each hybridization reaction was incubated at
72 47° C for 72 hours, and single-stranded capture libraries were recovered and PCR-amplified per
73 the manufacturer’s protocol. Post-capture library pools were sized and purified with AmpureXP
74 magnetic beads to remove residual primer-dimers and to enrich for a library fragment

75 distribution between 300 and 500bp, then diluted to 2nM prior to Illumina paired-end sequencing.
76 Paired end reads were trimmed with flexbar v 2.21 (params: --adapter CTTTGTGTTTGA - -
77 adapter-trim-end LEFT --nono-length-dist --threads 4 --adapter-min-overlap 7 --max- uncalled
78 150 --min-readlength 25) to remove single primer isothermal amplification adapter sequences
79 The resulting reads were analyzed with a pipeline that included Tophat v2.0.8 (params: --bowtie-
80 version = 2.1.0 for Ovation; --library-type fr-firststrand -- bowtie-version = 2.1.0 for Truseq) (2).
81 Expression levels (FPKM) were calculated with Cufflinks v2.0.2 (params--max-bundle-
82 length=10000000--num-threads 4). cDNA capture data was reviewed visually to evaluate the
83 expression of mutations identified by exome data and neoantigen prediction pipeline from
84 pVacSeq. Both cDNA-capture (Alt-read number) and FPKM values were considered for
85 candidate neoantigen prioritization.

86

87 ***HLA Typing:*** The subject's HLA type was determined by PCR-SSOP (ProImmune).

88

89 ***Neoantigen Identification.*** We developed a pipeline for the identification and prioritization of
90 potential neoantigens resulting from the somatic missense mutations detected from exome
91 sequencing analysis. Briefly, thresholds for filtering (binding- and coverage-based) using both
92 the exome and cDNA-cap sequencing data detailed above were used to compile a list of
93 expressed somatic missense mutations. Next, amino-acid substitutions corresponding to each of
94 the coding missense mutations were translated into a 21-mer amino acid FASTA sequence, with
95 10 amino acids flanking the substituted amino acid on each side. For each patient, these 21-mer
96 amino-acid sequences were evaluated through the HLA class I peptide-binding algorithm
97 NetMHC v3.2 (20,21) to identify high affinity neoantigens predicted to bind with high affinity to

98 the patient's HLA alleles. We similarly evaluated the corresponding wildtype sequences to
99 compare differences in predicted binding affinities, wherein any candidate neoantigens with a
100 predicted binding affinity IC₅₀ value < 500nm were considered for further evaluation. This
101 pipeline evolved into the pVAC-Seq pipeline (2) pipeline for identification of candidate
102 neoantigens.

103

104 **Sanger Sequencing of DNA samples:** DNA of patient PBMCs: xenograft and parental tumor
105 tissue was extracted with Qiagen QIAamp DNA Mini Kit and AllPrep DNA/RNA FFPE Kit,
106 respectively. Primers were designed with Primer-3. PCR reactions were carried out in 20 µl with
107 40 ng of DNA according to the manufactural recommendation of Phusion High-Fidelity DNA
108 Polymerase (ThermoFisher Scientific). PCR products were purified with QIAquick gel
109 extraction (QIAGEN) followed by sequencing (GeneWiz).

110

111 **Peptides.** Peptides were obtained lyophilized from Peptide 2.0 Inc. (> 95% purity), and were
112 dissolved in sterile water or in 10% DMSO dependent on the amino acid sequence.

113

114 **Mice.** NOD SCID gamma (NSG) mice were purchased from The Jackson Laboratory and housed
115 in a specific pathogen-free animal facility. All *in vivo* experiments used 8- to 12-week old female
116 NSG mice. All studies were performed in accordance with procedures approved by the
117 AAALAC accredited Animal Studies Committee of Washington University in St. Louis.

118

119 **Flow cytometry.** The following anti-human monoclonal antibodies (mAb) were used for cell
120 surface staining: CD3-APC-Cy7 (clone: OKT3), CD4-FITC (clone: OKT4), CD8-AF700 (clone:

121 SK1), CD45-BV785 (clone: HI30). All antibodies were obtained from BioLegend (San Diego,
122 CA). Samples were analyzed on an LSR Fortessa flow cytometer (BD Biosciences), and data
123 were analyzed using FlowJo software.

124

125 **Peptide binding assay.** Binding of synthetic peptides was assessed by measuring induction of
126 surface expression of HLA class I molecules: Peptide binding to several commonly expressed
127 human class I alleles was determined using T2 cells and genetically-modified T2 cells,
128 specifically T2-A3 (kindly provided by Dr. Storkus from UPMC/UPC) and T2-B7 cells (kindly
129 provided by Dr. Lutz, University of Kentucky). Following an established protocol (22) with a
130 few modifications, peptides (100 μ M) were incubated with T2, T2-A3 or T2-B7 cells in serum-
131 free RPMI at room temperature for one hour, then transferred to 28°C in a CO₂ incubator. The
132 following day, cells were stained with HLA allele-specific mAb (anti-HLA-A2 (BD
133 Pharmingen); anti-HLA-A3 (BD Pharmingen); and anti-HLA-B7 (provided by Dr. Ted Hansen),
134 and analyzed by flow cytometry.

135

136 **In vitro T cell analysis.** *In vitro* studies to evaluate the immunogenicity of candidate neoantigens
137 was performed using patients' autologous PBMC. Briefly, PBMC were cultured with individual
138 peptides corresponding to candidate neoantigens at 50 μ g/mL in RPMI with 5% human serum,
139 10 units/mL Penicillin-Streptomycin, 10 mM HEPES buffer, 2mM L-glutamine, 1 x non-
140 essential amino acid. IL2 (50 U/mL) was added every 2 days. Control PBMC were stimulated
141 with peptides corresponding to known viral antigens. On day 12, the peptide and tumor reactivity
142 of the T cells was determined by IFN γ ELISPOT assay. Cultured T cells were stimulated with
143 peptide-pulsed or autologous tumor-pulsed, irradiated autologous PBMC in the ELISPOT plate

144 followed by 20 hours incubation at 37°C. Developed spots were counted in an ELISPOT reader
145 (C.T.L., Shaker Heights, OH). In a different set of experiments, patients' PBMC were cultured
146 with irradiated autologous tumor cells instead of neoantigens for 12 days, as above. Tumor-
147 primed T cells were tested for recognition of neoantigens by IFN γ ELISPOT assay.

148

149 ***In vivo T-cell analysis.*** PDX tumor cells were subcutaneously injected into immunodeficient
150 NSG mice (1×10^6 cells per mouse). When tumors became palpable (around 3-4 mm in
151 dimension), 5×10^6 PBMC stimulated with prioritized neoantigens or control viral antigens were
152 transferred weekly into tumor-bearing NSG mice through tail vein injection (23-25). Mice were
153 observed daily and tumor size was measured every two days. In selected cases, PDX tumor-
154 bearing NSG mice were sacrificed at 30 days, and peripheral blood and tumor were harvested
155 from each mouse. Tumor tissue was processed into a single cell suspension through mechanical
156 (Miltenyi gentle MACS) and enzymatic dissociation followed by filtration through a 70 μ M cell
157 strainer. The single cell suspension and PBMC were stained for immune subsets followed by
158 flow cytometry. Functional analysis was performed by IFN γ ELISPOT assay using neoantigen
159 peptides identified from each patient.

160

161 ***Statistical analyses.*** Samples were compared using an unpaired, two-tailed Student's *t*-test,
162 unless specified.

163 RESULTS

164 To determine whether breast cancer neoantigens can be targeted with immunotherapy, we
165 established patient-derived xenografts from three patients with advanced breast cancer,
166 designated WHIM30, WHIM35, and WHIM37 (Supplementary Table S1 and Supplementary Fig
167 S1). We sequenced tumor and normal whole exomes and identified 2091 (WHIM30), 354
168 (WHIM35), and 235 (WHIM37) nonsynonymous single-nucleotide variant (SNV) mutations
169 using a published somatic variant pipeline (Table 1; Supplementary Tables S2-S4) (11). We
170 filtered the results of this pipeline analysis using stringent criteria for tumor and normal read
171 coverage, applying a minimal variant allele frequency (VAF) of 40%. This filter prioritized 74
172 (WHIM30), 33 (WHIM37), and 55 (WHIM37) candidate neoantigens from the dominant tumor
173 clone of the patient-derived xenografts. We next examined cDNA-capture sequencing from the
174 tumor RNA (3), to confirm that each mutant allele that was identified by our DNA-based
175 analysis was expressed in RNA, and to exclude any gene represented at fewer than 1 fragment
176 per kilobase of transcripts per million mapped reads (FPKM) (Supplementary Table S5). We also
177 generated HLA typing data for each patient using PCR-SSOP (Supplementary Table S6). We
178 selected nonsynonymous SNV mutations with a predicted binding affinity to the restricting HLA
179 alleles of < 500 nM. The final prioritized candidate neoantigens and their corresponding peptide
180 sequences (Supplementary Tables S7-S9) were pursued for further study.

181

182 Peptides corresponding to the candidate neoantigens were synthesized and assessed for binding
183 to the corresponding HLA class I allele using T2 cells (HLA-A02:01), and genetically modified
184 T2 cells expressing HLA-A03:01 or HLA-B07:02 (26). Of the 18 peptides tested, 15 (83%)
185 bound to the predicted HLA allele (Table 1; stabilization of MHC expression was measured by

186 flow cytometry, Supplementary Fig. S2). To evaluate the ability of autologous T cells to
187 recognize the candidate neoantigens *in vitro*, we cocultured peptides corresponding to the
188 candidate neoantigens with corresponding autologous PBMC for 12 days in the presence of IL2,
189 after which the T-cell response to each peptide was assessed in an IFN γ ELISPOT assay. Two of
190 nine (22%) WHIM30 candidate neoantigens (PALB2 and ROBO3) induced significant peptide-
191 specific T-cell responses ($*P < 0.05$, $**P < 0.01$, respectively) (Table 1; Fig. 1A). One of eight
192 (12.5%) WHIM35 candidate neoantigens (PTPRS), and one of eight (12.5%) WHIM 37
193 candidate neoantigens (ZDHHC16) also induced significant peptide-specific CD8⁺ T-cell
194 responses ($*P < 0.05$, $**P < 0.01$, respectively) (Table 1; Fig. 1B and C). The same candidate
195 neoantigens induced 1.6-3 times increased CD8⁺ T-cell responses compared with control
196 peptides after autologous mixed lymphocyte-tumor cultures using PBMC and irradiated PDX-
197 tumor cells (Supplementary Fig. S3).

198
199 To further characterize the specificity of the T-cell response to the prioritized breast cancer
200 neoantigens, we stimulated each patient's PBMC with peptides corresponding to the mutant
201 antigens for 12 days, then measured response to the antigens by IFN γ ELISPOT assays. Mutant
202 PALB2-stimulated T cells did not cross-react with wild-type PALB2 (Fig. 1D). A similar pattern
203 of reactivity was observed with the other breast cancer neoantigens: mutant, but not wild-type,
204 ROBO3 (Fig. 1D), PTPRS (Fig. 1E) and ZDHHC16 (Fig. 1F) induced T-cell responses. These
205 T-cell responses were not cross-reactive with the corresponding wild-type antigens. The
206 recognition of mutant antigens was HLA restricted, as both allele-specific and HLA class I
207 framework antibodies significantly reduced IFN γ secretion ($*P < 0.05$, $**P < 0.01$, respectively)
208 (Supplementary Fig. S4).

209

210 Two breast cancer neoantigens, PTPRS and ZDHHC16, are HLA-A02:01 restricted. We tested
211 the immunogenicity of these neoantigens in HHD mice. HHD mice are transgenic for a mutant
212 form of HLA-A2:01 that can interact with murine CD8 molecules, but they lack murine MHC
213 class I alleles. HHD mice were immunized with mutant PTPRS or ZDHHC16 peptide plus poly
214 I:C. The neoantigen-specific T-cell response was then measured by IFN γ ELISPOT. The mutant
215 PTPRS and ZDHHC16 peptides, but not other HLA-A02:01-specific breast cancer neoantigens,
216 induced a 3-6 times increased neoantigen-specific immune response (Supplementary Fig. S5).

217

218 To assess whether neoantigen-specific CD8⁺ T cells can recognize tumors, PBMC cultured *in*
219 *vitro* in the presence of mutant peptides were tested for reactivity against autologous tumor cells
220 in IFN γ ELISPOT assays. Both PALB2- and ROBO3-specific T cells (WHIM30) recognized
221 WHIM30 tumor cells (Fig. 1A). Similarly, PTPRS-specific T cells (WHIM35) and ZDHHC16-
222 specific T cells (WHIM37) recognized WHIM35 and WHIM37 tumor cells, respectively (Fig.
223 1B and C). In contrast, PBMC cultured with control peptides, including an immunogenic peptide
224 derived from mammaglobin-A (27), an immunodominant viral peptide, or EML2, a HLA-
225 A02:01-binding but nonimmunogenic mutant peptide (WHIM30), did not recognize tumor cells.
226 PBMCs stimulated with control peptides were responsive to the control peptides, except peptide
227 EML2, which is a nonimmunogenic neoantigen. Thus, neoantigen-specific CD8⁺ T cells do
228 recognize their cognate tumors.

229

230 Breast cancer neoantigens might be useful as targets for personalized cancer vaccines or other
231 immunotherapeutic strategies. Here, we assessed whether neoantigen-specific CD8⁺ T cells are

232 associated with antitumor immunity *in vivo*. We began by implanting WHIM30 tumor sections
233 subcutaneously in immune-compromised NOD SCID gamma (NSG) mice. After tumors became
234 palpable, 5×10^6 – 10×10^6 autologous PBMC stimulated *in vitro* with PALB2, ROBO3 or
235 control CMV peptides were adoptively transferred into tumor-bearing mice. Adoptive transfer
236 was repeated every seven days. Tumor growth was measured every two days. Adoptive transfer
237 of autologous PBMC stimulated with PALB2 and ROBO3 was associated with decreased tumor
238 growth, whereas adoptive transfer of PBMC stimulated with CMV had no impact on tumor
239 growth (Fig. 2A and C). Adoptive transfer of autologous PBMC from patient WHIM35
240 stimulated *in vitro* with PTPRS but not FluM1 peptide decreased WHIM 35 tumor growth
241 ($P < 0.05$) (Fig. 2B and D).

242

243 To understand the mechanism of action of tumor rejection following adoptive transfer, we
244 isolated tumor-infiltrating lymphocytes (TILs) from rejecting tumors and assayed them *ex vivo*
245 by IFN γ ELISPOT. TILs from rejecting WHIM30 tumors generated IFN γ in response to both
246 mPALB2 and mROBO3 (Fig. 2E). TILs from rejecting WHIM 35 tumors generated IFN γ in
247 response to mPTPRS (Fig. 2F). In both cases, no response to control peptides was observed.
248 Phenotypic analysis of TIL confirmed the presence of neoantigen-stimulated T cells in rejecting
249 tumors. In contrast, no T cells were detectable in growing tumors following adoptive transfer of
250 control, viral antigen-stimulated T cells (Fig. 2G, 2H).

251

252 Sanger sequencing results showed that the PTPRS mutation (G to A) was present in the
253 WHIM35 parental tumor as well as in the WHIM35 PDX tumor, but not in the patient's PBMC. .

254 DNA degradation in parental WHIM 30 and WHIM37 tumors prevented detection of
255 neoantigens.

256 **DISCUSSION**

257 We have used next-generation sequencing and computational analysis to identify and prioritize
258 candidate breast cancer neoantigens. Some of these candidate neoantigens were recognized by
259 the immune system, thus presenting potential targets for cancer immunotherapy. Successful
260 design of precision vaccines for treatment of human cancer will depend on rapid identification
261 and prioritization of candidate neoantigens (1–4, 28–30). Based on the data presented here, we
262 have initiated two phase 1 clinical trials testing neoantigen DNA and synthetic long-peptide
263 vaccines in patients with triple-negative breast cancer (TNBC) (NCT02348320 and
264 NCT02427581, respectively).

265
266 TNBC lacks expression of estrogen receptor, progesterone receptor, and HER2, and follows an
267 aggressive clinical course. Clonal and mutational analysis of primary TNBC suggests that TNBC
268 is characterized by a higher mutational frequency than other breast cancer subtypes (31–33). The
269 relative abundance of somatic mutations in TNBC suggests that neoantigens are more likely to
270 be present in this breast cancer subtype. Here, we observed that WHIM30, derived from a patient
271 with TNBC, had over 2000 somatic mutations. We identified and credentialed two candidate
272 neoantigens using algorithms designed to prioritize neoantigens from the dominant tumor clone,
273 followed by *in vitro* and *in vivo* immune assays. WHIM35 and WHIM37 are luminal subtype
274 breast cancers, with correspondingly lower mutational loads than WHIM30. Nonetheless, we
275 identified and credentialed neoantigens in both these tumors, consistent with recent reports that
276 human tumors containing limited mutations harbor neoantigens that can be targeted by immune
277 therapies (34).

278

279 The limited number of neoantigens identified in TNBC may be a shortcoming of our
280 identification process or may be related to the underlying biology of TNBC. Our sequencing and
281 epitope prediction algorithms are similar to those of other investigators: we identified somatic
282 missense mutations through exome sequencing of tumor and normal tissue, followed by
283 expression analysis by RNA sequencing, as many mutations are not expressed. Our final step
284 towards identification of candidate neoantigens involved the use of computer algorithms that
285 predict which mutations can give rise to peptides that can be presented by the patient's HLA
286 alleles (30,35,36). Preclinical studies performed to date suggest that the majority of candidate
287 neoantigens, i.e. those that are expressed and predicted to bind with high affinity, do not trigger
288 detectable T-cell responses. For example, of the top 62 predicted binding epitopes, only 2
289 conferred tumor rejection in a mouse sarcoma model (1). Likewise, Verdegaal et al. (37)
290 identified 501 and 226 non-synonymous mutations in two patients with advanced melanoma,
291 respectively, but only 2/501 and 3/226 triggered antigen-specific CD8⁺ T cells. Relevant data
292 from human breast cancers are not readily available. In the studies presented here we validated
293 one or two neoantigens per patient out of eight to nine candidate neoantigens in the dominant
294 tumor clone. Although the number of validated neoantigens is similar to that in other studies, the
295 number of candidate neoantigens is substantially lower. We used a stringent variant allele
296 frequency of 40%; lowering this number increases the number of candidate neoantigens.

297

298 It is too early to assess the clinical importance of targeting neoantigens. Immune therapy has
299 heretofore emphasized induction or enhancement of immune responses to tumor-associated
300 antigens such as HER2, MUC1, mammaglobin-A, and others (38,39). Although clinical
301 responses have been observed with vaccines targeting tumor-associated breast cancer antigens

302 (27,38,40), there is also evidence for a positive correlation between the number of candidate
303 neoantigens and patient survival (41). Perhaps targeting a combination of both types of antigens
304 will confer the greatest clinical benefit.

305

306 Our results support targeting neoantigens using vaccine-based immunotherapy in breast cancer.
307 Although cancer neoantigens are targets for immune checkpoint-inhibitor therapies (1,42), we
308 here show their concurrent value for personalized vaccine therapy, extending the results obtained
309 in a murine sarcoma model (1). Personalized vaccine therapy may provide many of the benefits
310 of immune checkpoint inhibitor therapy with decreased risk of autoimmunity and other severe
311 adverse events. Finally, our studies suggest that a combination of genomic, computational, and *in*
312 *vitro* functional assays can be used to identify, prioritize, and validate candidate breast cancer
313 neoantigens, thereby facilitating clinical translation of this approach.

ACKNOWLEDGEMENTS

We thank Dr. Robert Schreiber for his comments, suggestions, and support. We thank Dr. Matthew Gubin for technical advice. We thank the staff at the McDonnell Genome Institute for their expertise and support. We thank Dr. Seth D. Crosby and Chris Sawyer from the Genome Technology Access Center for technical consultant and expertise input.

REFERENCES

1. Gubin MM, Zhang X, Schuster H, Caron E, Ward JP, Noguchi T, *et al.* Checkpoint blockade cancer immunotherapy targets tumour-specific mutant antigens. *Nature* **2014**;515(7528):577-81 doi 10.1038/nature13988.
2. Hundal J, Carreno BM, Petti AA, Linette GP, Griffith OL, Mardis ER, *et al.* pVAC-Seq: A genome-guided in silico approach to identifying tumor neoantigens. *Genome Med* **2016**;8(1):11 doi 10.1186/s13073-016-0264-5
10.1186/s13073-016-0264-5 [pii].
3. Matsushita H, Vesely MD, Koboldt DC, Rickert CG, Uppaluri R, Magrini VJ, *et al.* Cancer exome analysis reveals a T-cell-dependent mechanism of cancer immunoediting. *Nature* **2012**;482(7385):400-4 doi 10.1038/nature10755.
4. Carreno BM, Magrini V, Becker-Hapak M, Kaabinejadian S, Hundal J, Petti AA, *et al.* A dendritic cell vaccine increases the breadth and diversity of melanoma neoantigen-specific T cells. *Science* **2015** doi 10.1126/science.aaa3828.
5. Alexandrov LB, Nik-Zainal S, Wedge DC, Aparicio SA, Behjati S, Biankin AV, *et al.* Signatures of mutational processes in human cancer. *Nature* **2013**;500(7463):415-21 doi 10.1038/nature12477.
6. Lawrence MS, Stojanov P, Mermel CH, Robinson JT, Garraway LA, Golub TR, *et al.* Discovery and saturation analysis of cancer genes across 21 tumour types. *Nature* **2014**;505(7484):495-501 doi nature12912 [pii]
10.1038/nature12912.
7. van Rooij N, van Buuren MM, Philips D, Velds A, Toebes M, Heemskerk B, *et al.* Tumor exome analysis reveals neoantigen-specific T-cell reactivity in an ipilimumab-responsive melanoma. *J Clin Oncol* **2013**;31(32):e439-42 doi 10.1200/JCO.2012.47.7521.
8. Robbins PF, Lu YC, El-Gamil M, Li YF, Gross C, Gartner J, *et al.* Mining exomic sequencing data to identify mutated antigens recognized by adoptively transferred tumor-reactive T cells. *Nat Med* **2013**;19(6):747-52 doi 10.1038/nm.3161.
9. Wolfel T, Hauer M, Schneider J, Serrano M, Wolfel C, Klehmann-Hieb E, *et al.* A p16INK4a-insensitive CDK4 mutant targeted by cytolytic T lymphocytes in a human melanoma. *Science* **1995**;269(5228):1281-4.
10. Li S, Shen D, Shao J, Crowder R, Liu W, Prat A, *et al.* Endocrine-therapy-resistant ESR1 variants revealed by genomic characterization of breast-cancer-derived xenografts. *Cell Rep* **2013**;4(6):1116-30 doi S2211-1247(13)00463-4 [pii]
10.1016/j.celrep.2013.08.022.
11. Griffith M, Griffith OL, Smith SM, Ramu A, Callaway MB, Brummett AM, *et al.* Genome Modeling System: A Knowledge Management Platform for Genomics. *PLoS Comput Biol* **2015**;11(7):e1004274 doi 10.1371/journal.pcbi.1004274
PCOMPBIOL-D-14-02043 [pii].
12. Li H, Durbin R. Fast and accurate short read alignment with Burrows-Wheeler transform. *Bioinformatics* **2009**;25(14):1754-60 doi btp324 [pii]
10.1093/bioinformatics/btp324.

13. Li H, Handsaker B, Wysoker A, Fennell T, Ruan J, Homer N, *et al.* The Sequence Alignment/Map format and SAMtools. *Bioinformatics* **2009**;25(16):2078-9 doi btp352 [pii]
10.1093/bioinformatics/btp352.
14. Li H. A statistical framework for SNP calling, mutation discovery, association mapping and population genetical parameter estimation from sequencing data. *Bioinformatics* **2011**;27(21):2987-93 doi btr509 [pii]
10.1093/bioinformatics/btr509.
15. Larson DE, Harris CC, Chen K, Koboldt DC, Abbott TE, Dooling DJ, *et al.* SomaticSniper: identification of somatic point mutations in whole genome sequencing data. *Bioinformatics* **2012**;28(3):311-7 doi btr665 [pii]
10.1093/bioinformatics/btr665.
16. Koboldt DC, Chen K, Wylie T, Larson DE, McLellan MD, Mardis ER, *et al.* VarScan: variant detection in massively parallel sequencing of individual and pooled samples. *Bioinformatics* **2009**;25(17):2283-5 doi btp373 [pii]
10.1093/bioinformatics/btp373.
17. Koboldt DC, Zhang Q, Larson DE, Shen D, McLellan MD, Lin L, *et al.* VarScan 2: somatic mutation and copy number alteration discovery in cancer by exome sequencing. *Genome Res* **2012**;22(3):568-76 doi gr.129684.111 [pii]
10.1101/gr.129684.111.
18. Saunders CT, Wong WS, Swamy S, Becq J, Murray LJ, Cheetham RK. Strelka: accurate somatic small-variant calling from sequenced tumor-normal sample pairs. *Bioinformatics* **2012**;28(14):1811-7 doi bts271 [pii]
10.1093/bioinformatics/bts271.
19. Cabanski CR, Magrini V, Griffith M, Griffith OL, McGrath S, Zhang J, *et al.* cDNA hybrid capture improves transcriptome analysis on low-input and archived samples. *J Mol Diagn* **2014**;16(4):440-51 doi S1525-1578(14)00072-5 [pii]
10.1016/j.jmoldx.2014.03.004.
20. Nielsen M, Lundegaard C, Worning P, Lauemoller SL, Lamberth K, Buus S, *et al.* Reliable prediction of T-cell epitopes using neural networks with novel sequence representations. *Protein Sci* **2003**;12(5):1007-17 doi 10.1110/ps.0239403.
21. Lundegaard C, Lamberth K, Harndahl M, Buus S, Lund O, Nielsen M. NetMHC-3.0: accurate web accessible predictions of human, mouse and monkey MHC class I affinities for peptides of length 8-11. *Nucleic Acids Res* **2008**;36(Web Server issue):W509-12 doi gkn202 [pii]
10.1093/nar/gkn202.
22. Hansen T, Myers N. Peptide induction of surface expression of class I MHC. *Curr Protoc Immunol* **2003**;Chapter 18:Unit 18 1 doi 10.1002/0471142735.im1811s57.
23. Stromnes IM, Schmitt TM, Chapuis AG, Hingorani SR, Greenberg PD. Re-adapting T cells for cancer therapy: from mouse models to clinical trials. *Immunol Rev* **2014**;257(1):145-64 doi 10.1111/imr.12141.
24. Eberlein TJ, Rosenstein M, Rosenberg SA. Regression of a disseminated syngeneic solid tumor by systemic transfer of lymphoid cells expanded in interleukin 2. *J Exp Med* **1982**;156(2):385-97.

25. Rosenberg SA, Restifo NP, Yang JC, Morgan RA, Dudley ME. Adoptive cell transfer: a clinical path to effective cancer immunotherapy. *Nat Rev Cancer* **2008**;8(4):299-308 doi nrc2355 [pii]
10.1038/nrc2355.
26. Elvin J, Potter C, Elliott T, Cerundolo V, Townsend A. A method to quantify binding of unlabeled peptides to class I MHC molecules and detect their allele specificity. *J Immunol Methods* **1993**;158(2):161-71.
27. Tiriveedhi V, Tucker N, Herndon J, Li L, Sturmoski M, Ellis M, *et al.* Safety and preliminary evidence of biologic efficacy of a mammaglobin-a DNA vaccine in patients with stable metastatic breast cancer. *Clin Cancer Res* **2014**;20(23):5964-75 doi 20/23/5964 [pii]
10.1158/1078-0432.CCR-14-0059.
28. Castle JC, Kreiter S, Diekmann J, Lower M, van de Roemer N, de Graaf J, *et al.* Exploiting the mutanome for tumor vaccination. *Cancer Res* **2012**;72(5):1081-91 doi 10.1158/0008-5472.CAN-11-3722.
29. Yadav M, Jhunjunwala S, Phung QT, Lupardus P, Tanguay J, Bumbaca S, *et al.* Predicting immunogenic tumour mutations by combining mass spectrometry and exome sequencing. *Nature* **2014**;515(7528):572-6 doi 10.1038/nature14001.
30. Zhang X, Sharma PK, Peter Goedegebuure S, Gillanders WE. Personalized cancer vaccines: Targeting the cancer mutanome. *Vaccine* **2016** doi S0264-410X(16)30399-1 [pii]
10.1016/j.vaccine.2016.05.073.
31. Liedtke C, Bernemann C, Kiesel L, Rody A. Genomic profiling in triple-negative breast cancer. *Breast Care (Basel)* **2013**;8(6):408-13 doi 10.1159/000357534 brc-0008-0408 [pii].
32. Shah SP, Roth A, Goya R, Oloumi A, Ha G, Zhao Y, *et al.* The clonal and mutational evolution spectrum of primary triple-negative breast cancers. *Nature* **2012**;486(7403):395-9 doi nature10933 [pii]
10.1038/nature10933.
33. Ding L, Ellis MJ, Li S, Larson DE, Chen K, Wallis JW, *et al.* Genome remodelling in a basal-like breast cancer metastasis and xenograft. *Nature* **2010**;464(7291):999-1005 doi 10.1038/nature08989.
34. Tran E, Turcotte S, Gros A, Robbins PF, Lu YC, Dudley ME, *et al.* Cancer immunotherapy based on mutation-specific CD4+ T cells in a patient with epithelial cancer. *Science* **2014**;344(6184):641-5 doi 10.1126/science.1251102.
35. Kakimi K, Karasaki T, Matsushita H, Sugie T. Advances in personalized cancer immunotherapy. *Breast Cancer* **2017**;24(1):16-24 doi 10.1007/s12282-016-0688-1.
36. Schumacher TN, Schreiber RD. Neoantigens in cancer immunotherapy. *Science* **2015**;348(6230):69-74 doi 10.1126/science.aaa4971.
37. Verdegaal EM, de Miranda NF, Visser M, Harryvan T, van Buuren MM, Andersen RS, *et al.* Neoantigen landscape dynamics during human melanoma-T cell interactions. *Nature* **2016**;536(7614):91-5 doi 10.1038/nature18945.

38. Sanchez K, Page D, McArthur HL. Immunotherapy in breast cancer: An overview of modern checkpoint blockade strategies and vaccines. *Curr Probl Cancer* **2016**;40(2-4):151-62 doi 10.1016/j.currproblcancer.2016.09.009.
39. Li L, Goedegebuure P, Mardis ER, Ellis MJ, Zhang X, Herndon JM, *et al.* Cancer genome sequencing and its implications for personalized cancer vaccines. *Cancers (Basel)* **2011**;3(4):4191-211 doi 10.3390/cancers3044191.
40. Clifton GT, Mittendorf EA, Peoples GE. Adjuvant HER2/neu peptide cancer vaccines in breast cancer. *Immunotherapy* **2015**;7(11):1159-68 doi 10.2217/imt.15.81.
41. Brown SD, Warren RL, Gibb EA, Martin SD, Spinelli JJ, Nelson BH, *et al.* Neo-antigens predicted by tumor genome meta-analysis correlate with increased patient survival. *Genome Res* **2014**;24(5):743-50 doi 10.1101/gr.165985.113.
42. Rizvi NA, Hellmann MD, Snyder A, Kvistborg P, Makarov V, Havel JJ, *et al.* Mutational landscape determines sensitivity to PD-1 blockade in non-small cell lung cancer. *Science* **2015** doi 10.1126/science.aaa1348.

Figure Legends:

Fig. 1. Identification and validation of candidate neoantigens. Autologous PBMCs were stimulated with candidate breast cancer neoantigens for 12 days. CD8⁺ T-cell IFN γ ELISPOT assays were performed on day 12 by co-culturing stimulated PBMC overnight with autologous, irradiated PBMCs pulsed with the candidate neoantigens (black) or irradiated PDX tumor cells (white). The immune response induced by candidate neoantigens and PDX tumor cells is shown in (A) WHIM30, (B) WHIM35 and (C) WHIM37. Negative controls in the ELISPOT assays included responder T cells cultured with no peptide (number of spot forming cells per 10⁶ cells was 50-120) or irrelevant peptide (number of spot forming cells per 10⁶ cells was 250-400). The background with irrelevant peptide was subtracted from the experimental condition in each case. To confirm the specificity of the immune response induced by candidate neoantigens, CD8⁺ T-cell IFN γ ELISPOT assays were performed against mutant (black) and wildtype peptides (white) after 12 day stimulation with mutant peptides. The results are shown in (D) WHIM30, (E)

WHIM35 and (F) WHIM37. Data are presented as means \pm s.e.m ($n = 3$ wells per peptide in ELISpot assay) and are representative of three independent experiments. Samples were compared using unpaired, two tailed Student's test ($*P < 0.05$, $** P < 0.01$), SFC is spot forming cells.

Fig. 2. Adoptive transfer of neoantigen-stimulated T cells inhibits growth of PDXs *in vivo*.

PDXs were established by injection of 1×10^6 tumor cells subcutaneously into NSG mice. $5-10 \times 10^6$ neoantigen-stimulated T cells and control viral-antigen stimulated T cells were adoptively transferred into tumor-bearing mice after the tumor became palpable. T cells were transferred at days 0, 7, and 14. Tumor size was measured every two days. (A) WHIM30 tumor growth following treatment with PBMC stimulated with mutant PALB2/ROBO3 (black solid circle) or CMV peptides (black solid square). (B) WHIM35 tumor growth following treatment with PBMC stimulated with mutant PTPRS (black solid circle) or FluM1 peptides (black solid square). (A) and (B) Data are presented as tumor size (mm^2) \pm s.e.m. of 5 mice per group ($*P < 0.05$). (C) WHIM30 tumor size (52 days after tumor challenge) following treatment with PBMC stimulated with mutant PALB2/ROBO3 or CMV peptides. (D) WHIM35 tumor size (62 days after tumor challenge) following treatment with PBMC stimulated with mutant PTPRS or CMV peptides. (E, G) TILs were isolated from WHIM30 tumors following treatment with PBMC stimulated with mutant PALB2/ROBO3 (black) or negative control mutant E1F5B and CMV (white) peptides. CD8^+ T-cell $\text{IFN}\gamma$ ELISPOT assay and flow cytometry were performed with experimental and control peptides as indicated. (F, H) TILs were isolated from WHIM30 tumors following treatment with PBMC stimulated with mutant PTPRS (black) or negative control mutant EML2 and FluM1 peptides (white). CD8^+ T-cell $\text{mIFN}\gamma$ ELISPOT assay and flow cytometry were

performed with experimental and control peptides as indicated. (E) and (F) Data shown are mean \pm s.e.m ($n = 3$ wells per peptide in ELISpot assay). Data shown are representative of three independent experiments. Samples were compared using an unpaired, two-tailed Student t test ($P < 0.05$).

Table 1.

Patient	Number of Tier 1 mutations†	Number of mutations expressed‡	Number predicted to bind§	Number actually binding/tested*	Number immunogenic in vitro**	Number conferring tumor recognition***
WHIM30	2091	15	9	7/8	2/9	2/2
WHIM35	354	8	8	3/3	1/7	1/1
WHIM37	235	11	8	6/8	1/8	1/1

Table 1. Overview of identified neoantigens

† As determined by whole-exome sequencing and (see Supplementary Methods) from each patient xenograft.

‡ As determined by cDNA Cap-Seq and other filters described in Supplementary Methods.

§ As determined by NetMHC 3.2 (affinity of mutant peptides < 500 nM).

• Binding assay evaluated using the T2 assay (see Supplementary Methods).

** Reactivity as determined by IFN- γ ELISPOT assay *in vitro* as described in Supplementary Methods.

*** Reactivity as determined by tumor growth inhibition in NSG mouse model *in vivo* as described in Supplementary Methods.

Published Online First June 15, 2017; DOI: 10.1158/2326-6066.CCR-16-0264

Fig. 1.

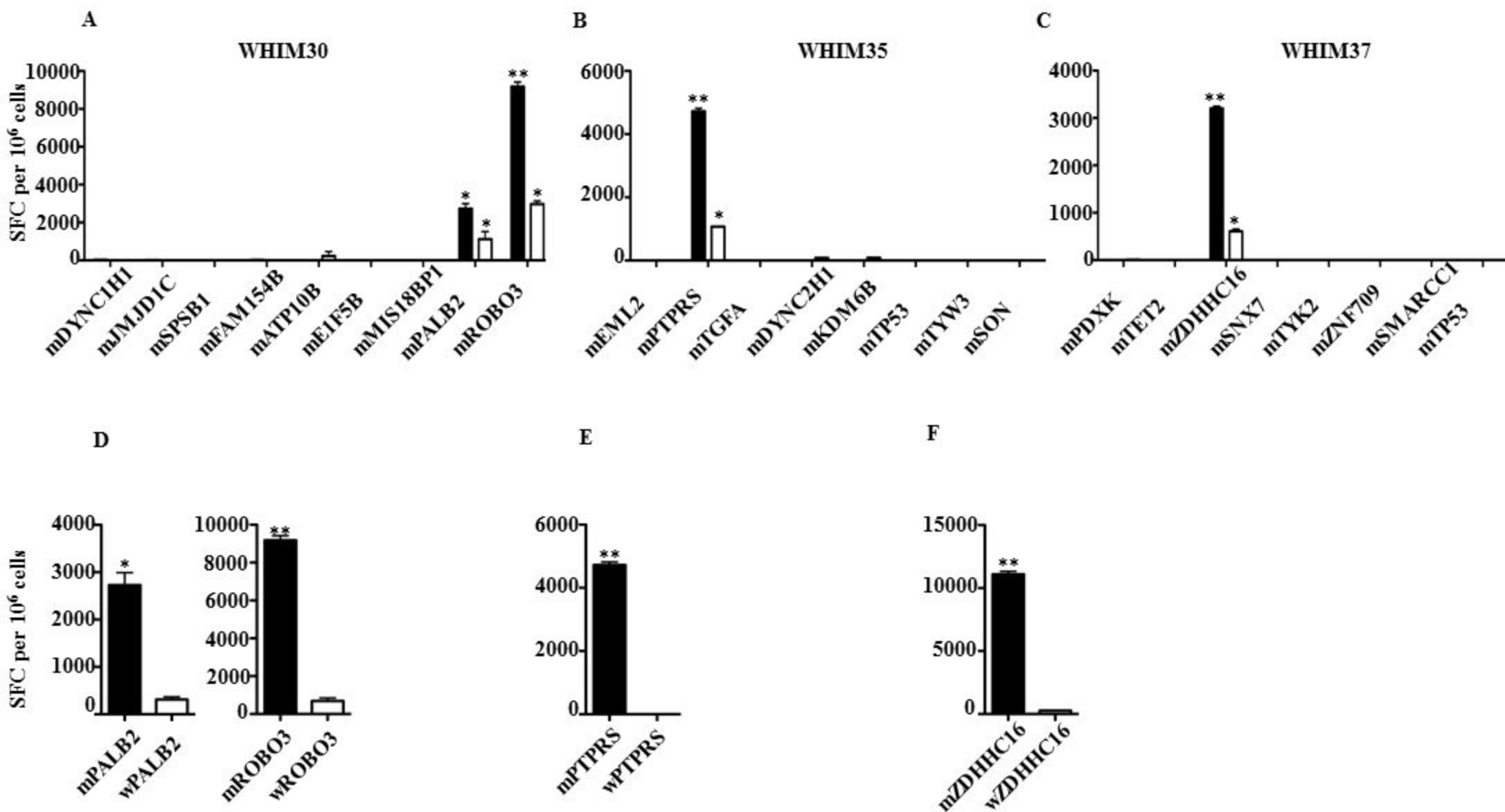
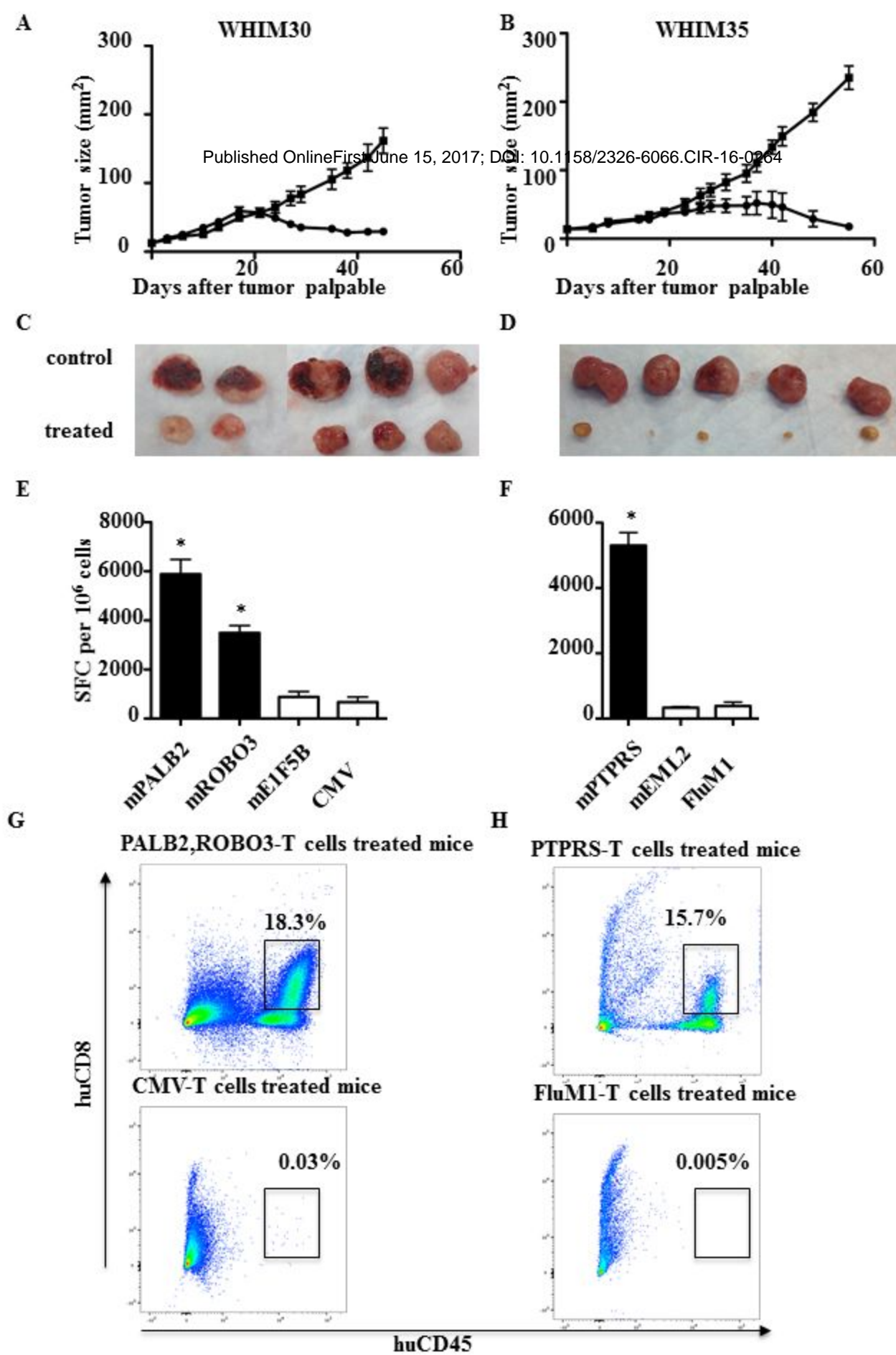


Fig. 2.



Cancer Immunology Research

Breast cancer neoantigens can induce CD8 T cell responses and antitumor immunity

Xiuli Zhang, Samuel Kim, Jasreet Hundal, et al.

Cancer Immunol Res Published OnlineFirst June 15, 2017.

Updated version	Access the most recent version of this article at: doi: 10.1158/2326-6066.CIR-16-0264
Supplementary Material	Access the most recent supplemental material at: http://cancerimmunolres.aacrjournals.org/content/suppl/2017/06/14/2326-6066.CIR-16-0264.DC1

E-mail alerts	Sign up to receive free email-alerts related to this article or journal.
----------------------	--

Reprints and Subscriptions	To order reprints of this article or to subscribe to the journal, contact the AACR Publications Department at pubs@aacr.org .
-----------------------------------	--

Permissions	To request permission to re-use all or part of this article, use this link http://cancerimmunolres.aacrjournals.org/content/early/2017/06/14/2326-6066.CIR-16-0264 . Click on "Request Permissions" which will take you to the Copyright Clearance Center's (CCC) Rightslink site.
--------------------	--